

Adhesion behavior between yttrium-stabilized zirconia added $\text{La}_{0.8}\text{Ca}_{0.2}\text{Cr}_{0.9}\text{Co}_{0.1}\text{O}_{3-\delta}$ interconnector and yttrium-stabilized zirconia-based substrate

Ho-Chang Lee^a, Bo-Kyung Kang^a, Joon-Hyung Lee^a, Young-Woo Heo^a, Jae-Yuk Kim^b,
Jeong-Joo Kim^{a,*}

^a*School of Materials Science and Engineering, Kyungpook National University, Daegu 702–701, Republic of Korea*

^b*Ssangyong Materials Corp., Daegu 704–832, Republic of Korea*

Received 28 February 2013; received in revised form 16 April 2013; accepted 16 April 2013

Available online 22 April 2013

Abstract

Because of the different densification characteristics of a $\text{La}_{0.8}\text{Ca}_{0.2}\text{Cr}_{0.9}\text{Co}_{0.1}\text{O}_{3-\delta}$ (LCCC) interconnector and a NiO added yttrium-stabilized zirconia (YSZ) anode, complete adhesion between the two layers is hardly obtainable. In this study, we have investigated the sintering behavior of LCCC with the addition of YSZ. As the amount of YSZ increases, densification of the LCCC is inhibited and the initial temperature of the densification increases. However, when the LCCC–YSZ composite layer is screen printed on the NiO–YSZ substrates, the density of the composite layer increases and the layer is firmly attached to the substrates. It is proposed that tensile stress is decreased on the composite layer due to the relatively delayed densification of the LCCC–YSZ composite, compared to the densification of the NiO–YSZ substrate.
© 2013 Elsevier Ltd and Techna Group S.r.l. All rights reserved.

Keywords: A. Sintering; B. Composite; Adhesion; Microstructure; Solid oxide fuel cell

1. Introduction

The basic elements of a solid oxide fuel cell (SOFC) are electrolytes, anodes, cathodes, and interconnectors. Each element serves its purpose and shall meet certain requirements. In particular, an interconnector must possess its own stability in the oxidizing and reducing media, chemical compatibility with other elements, and electrical conductivity. $\text{La}_{0.8}\text{Ca}_{0.2}\text{Cr}_{0.9}\text{Co}_{0.1}\text{O}_{3-\delta}$ (LCCC), which is used as an interconnector material for solid oxide fuel cells, should be gastight to prevent cross leakage of fuel and gases enriched in oxygen [1,2]. Therefore, it is required to have not only phase stability but also a dense microstructure, in an oxidation–reduction atmosphere. In order to increase the sintering density of LCCC, nano powders of LCCC with high driving force of sintering have been manufactured via the Pechini process [3], aqueous combustion process [4] and hydrothermal process [5]. There

has also been a study on increasing the density by changing the raw materials of calcium sources [6].

The interconnector layer is usually formed by screen printing and co-firing the LCCC on a pre-sintered NiO–YSZ (yttrium-stabilized zirconia) substrate. If there is a big difference in the shrinkage rate between the substrate and the LCCC layer, stress occurs at the interface during co-firing. Generally, because the thin interconnector layer is printed on a thick substrate with solidity, adjustment of the densification behavior of the interconnector material is believed to provide an easy way to improve adhesion between them. When the shrinkage rate of the LCCC layer is relatively larger than that of the substrate, the LCCC layer has tensile stress during co-firing. Therefore, there is a greater possibility of having low densification, cracks and delamination on the LCCC layer. In this case, as a problem solver, materials' properties could be engineered by employing the concept of composite as reported in previous studies [7,8].

In this study, different amounts of YSZ were added to the LCCC in order to adjust the densification behavior during sintering, and the microstructures of the LCCC–YSZ composites were examined. At the same time, the electrical conductivity of the

*Corresponding author. Tel.: +82 53 950 5635; fax: +82 53 950 5645.

E-mail address: jjkim@knu.ac.kr (J.-J. Kim).

sintered composites was also examined, in relation to changes in the microstructures. The LCCC–YSZ composite pastes were screen printed on the NiO–YSZ substrates and co-fired. The adhesion characteristics of the LCCC–YSZ layer on the NiO–YSZ substrates were analyzed. The results were explained on the basis of the decreased stress (stress adjustment) between the two layers during co-firing.

2. Experimental procedure

The raw materials of LCCC ($\text{La}_{0.8}\text{Ca}_{0.2}\text{Cr}_{0.9}\text{Co}_{0.1}\text{O}_{3-\delta}$, average particle size $\approx 0.28\mu\text{m}$, Kceracell, Korea) and 8 mol% yttrium-stabilized zirconia (8YSZ, 99.85%, average particle

size $\approx 1.45\mu\text{m}$, Unitec Ceramics, UK) were used for the interconnectors. The LCCC–8YSZ composites containing 0, 30, 40 and 50 wt% of 8YSZ were prepared by mild ball milling, using zirconia balls for 24 h in ethanol, and then the mixtures were dried at 80°C . After drying, the composite powders were formed into 15 mm diameter pellets by a sequential process of uniaxial pressing, followed by cold isostatic pressing (CIP). Subsequent CIP of the green compact was conducted at 100 MPa for 5 min. The composite pellets were sintered at 1400°C for 2 h in air.

Powder X-ray diffraction with nickel-filtered $\text{Cu-K}\alpha$ radiation (Panalytical, X'pert pro, Netherlands) was used for phase identification. For the lattice parameter measurement, a silicon standard powder (SRM 640B, NIST, USA) was added to the samples. The densification behavior of the composite pellets was analyzed with a TMA (TD5000SA, Bruker, Germany). The density of the sintered composites was determined by the Archimedes method, and the microstructure was observed by FE-SEM (JSM-6701F, JEOL, Japan). The 4-probe DC electrical characteristics of the composites were measured using a Galvanodynamic measurement system (VersaSTAT3, Princeton Applied Research, USA). The sample dimension for the electrical characterization was 13 mm (length) and 4.2 mm (diameter).

The NiO–YSZ substrate was prepared using raw materials of NiO (99.9%, Sumitomo, Japan) and 8YSZ (8 mol% Y_2O_3 doped ZrO_2 , 99.9%, Tosho, Japan) powders. The homogeneously mixed powder with a weight ratio of NiO:YSZ=56:44 was calcined at 1100°C , then extruded. The porosity of the substrate was estimated to be about 23.7%.

For the preparation of the composite pastes, the LCCC powder, ethyl cellulose and α -terpineol were mixed in ethanol with a weight ratio of 60:5:35. Then the pastes were printed on

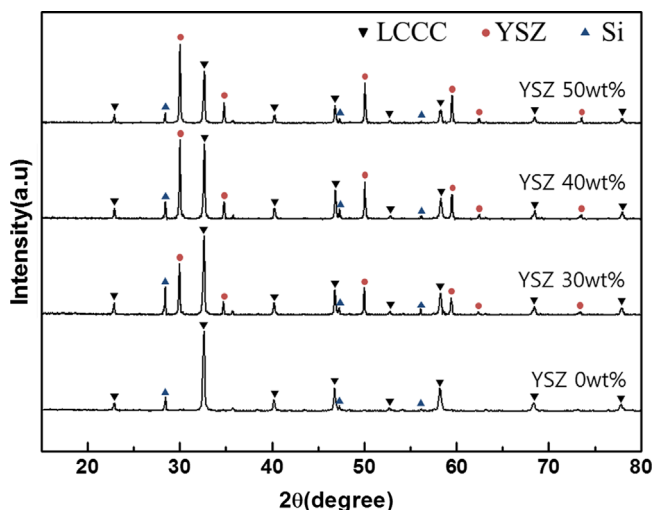


Fig. 1. X-ray diffraction patterns of the LCCC–YSZ composite samples sintered at 1400°C for 2 h as a function of the YSZ content.

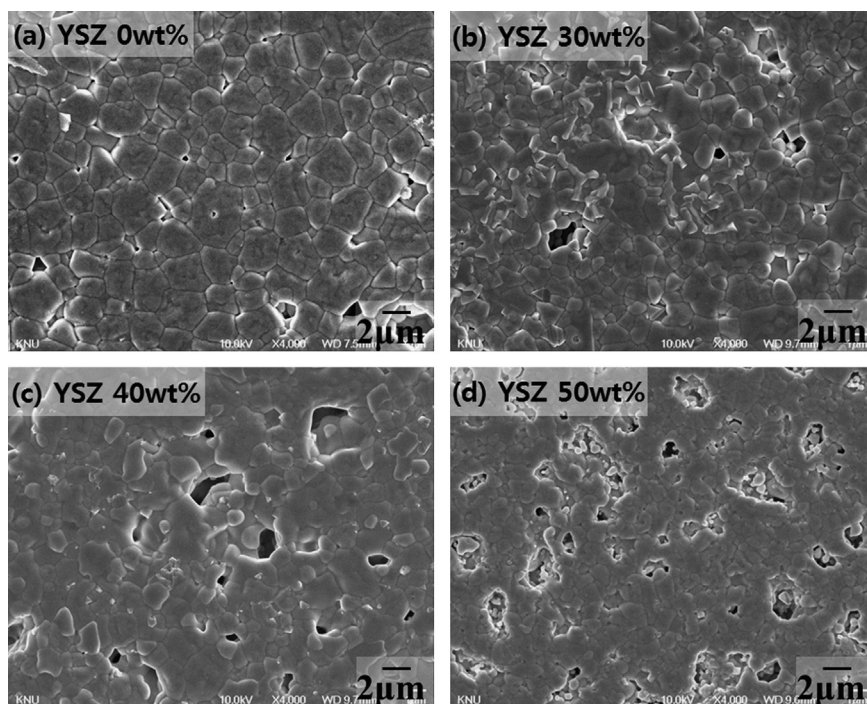


Fig. 2. The microstructures of the LCCC–YSZ composite pellets sintered at 1400°C for 2 h as a function of the YSZ content.

NiO–YSZ substrates using a 150 mesh screen. After drying, the bi-layer specimens were co-fired at 1400 °C for 4 h in air with a constant ramp up rate of 5 °C min⁻¹.

3. Results and discussion

Fig. 1 shows a series of X-ray diffraction patterns of the LCCC–YSZ composite samples sintered at 1400 °C for 2 h as a function of the YSZ content. The composite sample consists of the two components of the LCCC and YSZ, and the diffraction intensity originated from the YSZ increased as the content of YSZ increased. Even after sintering at a relatively high temperature of 1400 °C, no severe chemical reaction between the two components was observed. Therefore, the lattice constants were almost invariant.

Fig. 2 shows the microstructures of the LCCC–YSZ composite pellets sintered at 1400 °C for 2 h, with different amounts of YSZ contents. As the amount of YSZ was increased, the densification of the LCCC–YSZ composite was inhibited.

Porosity measured by the point counting method increased from 4.2% to 23.9%, as the amount of YSZ increased in the LCCC. De Jonghe et al.[9] examined the densification behavior of fine ZnO powder (particle size $\approx 0.4 \mu\text{m}$) with the addition of large SiC powder (particle size $\approx 14 \mu\text{m}$), and

reported that the inclusions lead to a drastic reduction in the densification of the composite relative to that of the pure ZnO matrix. This was because a hard second phase can severely limit the densification rates by generating a mean hydrostatic stress, which opposes the compressive sintering stress of the matrix, and the stress rapidly increases with the increased volume fraction of the second phase. The results of this study agree with the results of De Jonghe, in that the existence of the inclusion inhibits densification.

Fig. 3 shows the bulk density and electrical conductivity of the YSZ–LCCC composite pellets, sintered at 1400 °C for 2 h, as a function of the YSZ contents. As the amount of the YSZ increased, the bulk density decreased. This kind of density behavior is due to the increase in YSZ (6.048 g/cm³) in LCCC (6.234 g/cm³) and to the increase in porosity, shown in Fig. 2. In addition, the conductivity of 0.2 S cm⁻¹ for pure LCCC decreased as the amount of YSZ increased. When 50 wt% of YSZ was added, the conductivity of the LCCC decreased to 0.011 S cm⁻¹. This phenomenon is due to a decrease in the conduction paths between the LCCC (electrical conductor) grains, as the YSZ volume fraction (insulator) increases. Concerning the conductivity of the 50 wt% YSZ added sample at high temperature, it increased with temperature and reached about 16 S cm⁻¹ at 800 °C in air. The conductivity of (La_{1-x}Ca_x)(Cr_{1-y}Co_y)O₃ is dependent on the cationic ratios of the components. However, the conductivity values of LCCC for the use of SOFC is generally known to be about 25–47 S cm⁻¹ at 700–800 °C [6,10]. In spite of the large amount of the inclusion (50 wt% of YSZ) addition, the conductivity of 16 S cm⁻¹ at 800 °C deserves positive consideration for real application.

Fig. 4(a) shows a comparison of the densification behaviors of the LCCC–YSZ composite pellets as well as the NiO–YSZ substrate which was analyzed by TMA. In the case of the NiO–YSZ substrate, densification begins at around 1200 °C, and about 16.5% of shrinkage was observed when the temperature reached 1400 °C. On the other hand, when pure LCCC is sintered, densification begins at around 900 °C, and over 10% of the densification is already in progress at around 1200 °C, where the NiO–YSZ substrate begins to be densified. This result clearly shows that there is a wide gap in the temperature where the densification of the pure LCCC and the NiO–YSZ substrate begins.

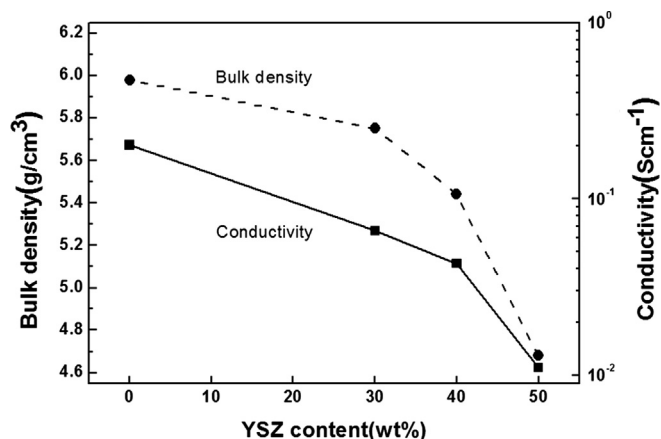


Fig. 3. The bulk density and the electrical conductivity of the YSZ–LCCC composite pellets, sintered at 1400 °C for 2 h, as a function of the YSZ contents.

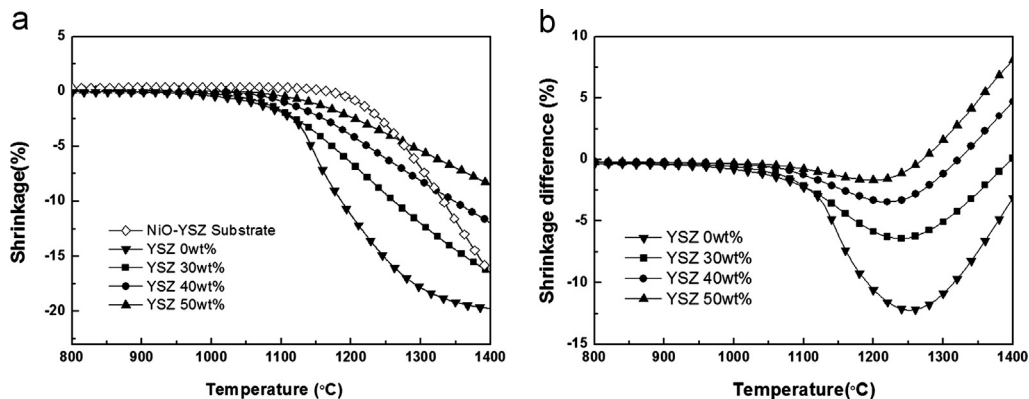


Fig. 4. (a) Shrinkage of the LCCC–YSZ composite pellets and the NiO–YSZ substrate, and (b) differences in shrinkage between the LCCCs and the NiO–YSZ substrate.

Fig. 4(b) shows the shrinkage differences between the LCCCs and the NiO–YSZ substrate, at each temperature. The shrinkage difference was evaluated from the shrinkage curves of the LCCCs and the substrate shown in Fig. 4(a), i.e., the shrinkage value of the substrate minus that of the LCCCs. Therefore, a negative value for the shrinkage difference means that the shrinkage of the LCCC is relatively larger than that of the substrate. In this case, tensile stress occurs on

the LCCC layer, if the bi-layer of the LCCC and the substrate is co-fired. In contrast, if the shrinkage difference has a positive value, compressive stress occurs on it. In the case of the pure LCCC, the shrinkage difference was negative for the whole temperature range. A maximum shrinkage difference of 12.5% was observed at around 1250 °C, making it quite natural that good adhesion of the LCCC layer onto the NiO–YSZ substrate never occurs.

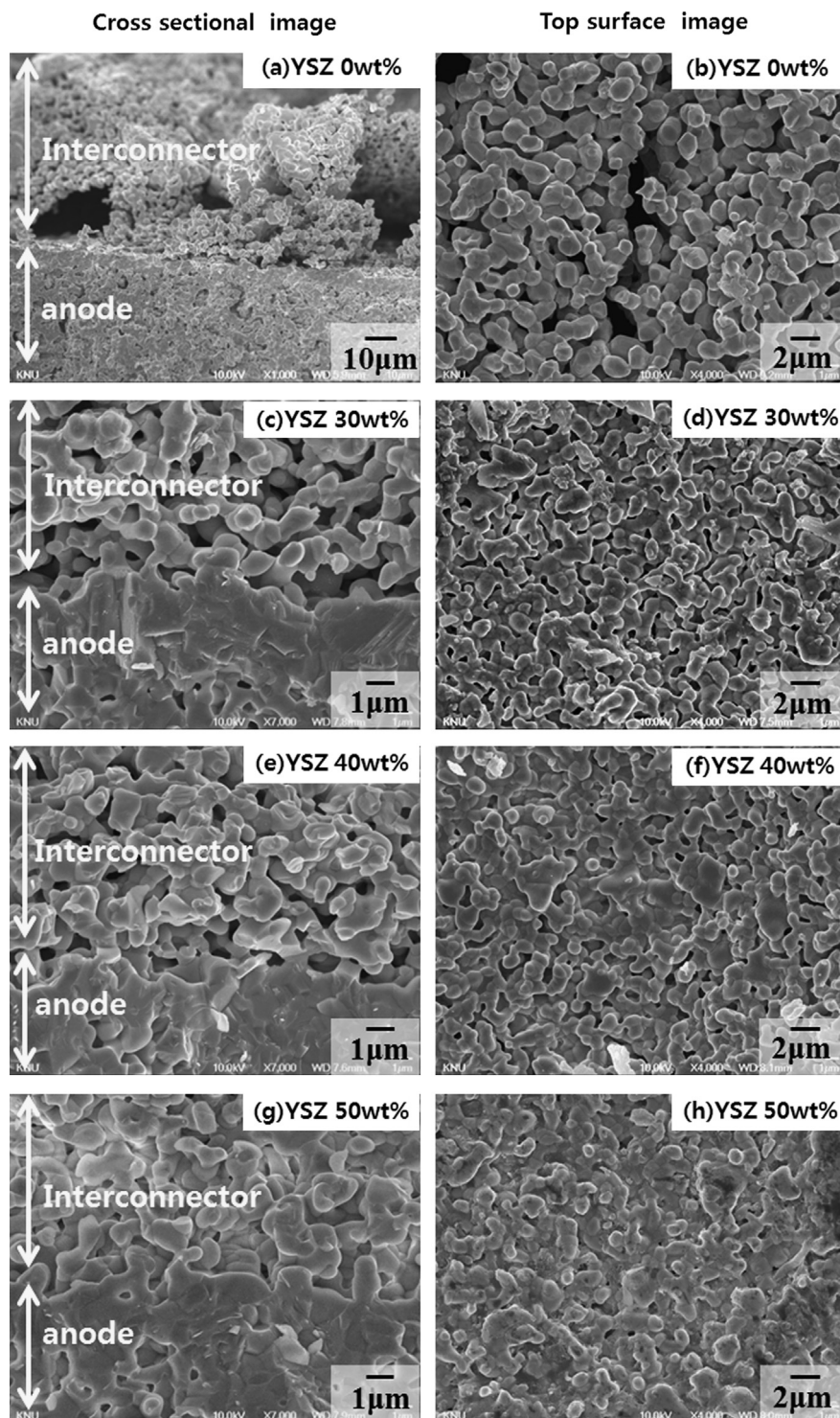


Fig. 5. The cross sectional SEM images of the bi-layers (left side) and those top surface images (right side). The bi-layers were co-fired at 1400 °C for 4 h.

When YSZ is added to LCCC, the gradient of the shrinkage curves decreased as more YSZ was added which had the effect of retarding densification shown in Fig. 4(a). The initial temperature of the densification increased as the amount of the YSZ increased, and densification at 1400 °C also decreased. Especially when the YSZ was added by 50 wt%, the initial temperature of sintering was around 1120 °C, and the densification was 8.4% at 1400 °C. This means the densification was more suppressed than the substrate. In the case of the 40 and 50 wt% of the YSZ added LCCCs, there were turn-over points from tensile to compressive stress as their shrinkage curves traverse the substrate's curve (Fig. 4(a)) and the shrinkage difference values changed from negative to positive (Fig. 4(b)).

Fig. 5 shows the adhesion characteristics of the LCCC–YSZ composite layer on the substrate. The LCCC–YSZ composite pastes were screen printed on the NiO–YSZ substrate and co-fired at 1400 °C for 4 h. The cross sectional images of the bi-layers are on the left side while the top surface image is shown on the right side. (a) is the image of the pure LCCC layer on the NiO–YSZ substrates and the occurrence of delamination was observed on the interface between the LCCC and NiO–YSZ substrate. (b) is the top surface image of the pure LCCC screen printed on the NiO–YSZ. It was more porous compared to Fig. 2(a), and cracks were also observed on it. Jagota [11,12] reported that in-plane tensile stress can cause crack-like defects and porous channels in the constrained film or delamination from the substrate. This phenomenon supports the fact that the stress between the LCCC layer and the substrate actually affect the microstructure development, which was mentioned in Fig. 4(b). The microstructure of the LCCC–YSZ composite samples are shown in (c) and (d) with the 30 wt% of YSZ, (e) and (f) with the 40 wt% of YSZ, and (g) and (h) with the 50 wt% of YSZ. As the YSZ increased, adhesion and densification of the LCCCs also increased.

The improved adhesion between the LCCC–YSZ composite layers and the NiO–YSZ substrate can be explained by a reduction in stress at the interface of the two layers. From the perspective of pure LCCC, it is regarded that more compressive stress is applied (tensile stress decreases) to the LCCC layer along with an increase in the YSZ content which leads to denser microstructures of the LCCC layers as well as improved adhesion. On the other hand, because the LCCC–YSZ composite and the NiO–YSZ substrate have the same component of YSZ, the improved adhesion also might be considered an effect of the increased content of YSZ in LCCCs.

4. Conclusions

Different amounts of YSZ were added to LCCC, and the sintering behavior of the LCCC–YSZ composite was examined. As the amount of YSZ increased in the LCCC, densification of the composite was retarded and the electric conductivity decreased. However, when the LCCC–YSZ composite is screen printed on the NiO–YSZ substrate and

co-fired, densification of the composite increased and adhesion also improved as the amount of YSZ increased. The result of the densification of the composite layer on the substrate is opposite to the case of the composite sintered alone.

TMA monitoring predicted that there would be great tensile stress on the LCCC interconnector side when the LCCC layer on the NiO–YSZ substrate is co-fired. The tensile stress on the LCCC layer, which negatively affects the densification, could decrease and eventually switch to compressive stress from the amount of the YSZ. The improved densification and adhesion of the LCCC composite layer are explained by the stress adjustment during sintering with the addition of YSZ.

Acknowledgments

This research was financially supported by the Ministry of Education, Science Technology (MEST) and National Research Foundation of Korea(NRF) through the Human Resource Training Project for Regional Innovation. This work was supported by the National Research Foundation of Korea Grant (2011-0012678, 2009-0093819) funded by the Korean Government.

References

- [1] W.Z. Zhu, S.C. Deevi, Development of interconnect materials for solid oxide fuel cells, *Materials Science and Engineering: A* 348 (2003) 227–243.
- [2] J. Molenda, K. Swierczek, W. Zajac, Functional materials for the IT-SOFC, *Journal of Power Sources* 173 (2007) 657–670.
- [3] M. Mori, N.M. Sammes, Sintering and thermal expansion characterization of Al-doped and Co-doped lanthanum strontium chromites synthesized by the Pechini method, *Solid State Ionics* 146 (2002) 301–312.
- [4] K. Deshpande, A. Mukasyan, A. Varma, Aqueous combustion synthesis of strontium-doped lanthanum chromite ceramics, *Journal of the American Ceramic Society* 86 (2003) 1149–1154.
- [5] J. Ovenstone, K.C. Chan, C.B. Ponton, Hydrothermal processing and characterization of doped lanthanum chromite for use in SOFCs, *Journal of Materials Science* 37 (2002) 3315–3322.
- [6] S.T. Park, B.H. Choi, M.J. Ji, Y.T. An, H.J. Choi, Effects of Ca-source on the sintering and electrical properties of $\text{La}_{0.7}\text{Ca}_{0.3}\text{Cr}_{0.9}\text{Co}_{0.1}\text{O}_{3-\delta}$ for solid oxide fuel cell interconnects, *Journal of the Korean Ceramic Society* 48 (2011) 246–250.
- [7] J. Piao, K. Sun, N. Zhang, S. Xu, A study of process parameters of LSM and LSM–YSZ composite cathode films prepared by screen-printing, *Journal of Power Sources* 175 (2008) 288–295.
- [8] X. Zhou, P. Wang, L. Liu, K. Sun, Z. Gao, N. Zhang, Improved electrical performance and sintering ability of the composite interconnect $\text{La}_{0.7}\text{Ca}_{0.3}\text{CrO}_{3-\delta}/\text{Ce}_{0.8}\text{Nd}_{0.2}\text{O}_{1.9}$ for solid oxide fuel cells, *Journal of Power Sources* 191 (2009) 377–383.
- [9] L.C. De Jonghe, M.N. Rahaman, C.H. Hsueh, Transient stresses in bimodal compacts during sintering, *Acta Metallurgica* 34 (1986) 1467–1471.
- [10] W.Z. Zhu, S.C. Deevi, Development of interconnect materials for solid oxide fuel cells, *Materials Science and Engineering: A* 348 (2003) 227–243.
- [11] A. Jagota, C.Y. Hui, Mechanics of sintering thin films–II. Cracking due to self-stress, *Mechanics of Materials* 11 (1991) 221–234.
- [12] R.K. Bordia, A. Jagota, Crack growth and damage in constrained sintering films, *Journal of the American Ceramic Society* 76 (1993) 2475–2485.